NACA

RESEARCH MEMORANDUM

FREE-FLIGHT-TUNNEL INVESTIGATION OF THE LOW-SPEED STABILITY AND CONTROL CHARACTERISTICS OF A MODEL HAVING A FUSELAGE OF RELATIVELY FLAT CROSS SECTION

By John W. Paulson and Joseph L. Johnson, Jr.

Langley Aeronautical Laboratory
Langley Field, Va.

NATIONAL ADVISORY COMMITTEE
FOR AERONAUTICS

WASHINGTON

February 24, 1953

NATIONAL ADVISORY COMMITTEE FOR AERONAUTICS

RESEARCH MEMORANDUM

FREE-FLIGHT-TUNNEL INVESTIGATION OF THE LOW-SPEED STABILITY AND CONTROL CHARACTERISTICS OF A MODEL HAVING A FUSELAGE OF RELATIVELY FLAT CROSS SECTION

By John W. Paulson and Joseph L. Johnson, Jr.

SUMMARY

Since models having fuselages of relatively flat cross section have been found to possess unusual static stability characteristics, an experimental investigation has been made in the Langley free-flight tunnel to determine the low-speed stability and control characteristics of a model of this type. In flight, the model exhibited an erratic behavior in pitch and yaw, apparently because of random trim changes associated with the flow from the forward portion of the flat fuselage. The model had an unusually high maximum lift coefficient because of its flat-fuselage design, but the maximum lift coefficient that could be obtained in flight tests was limited because of low dynamic lateral stability and low static longitudinal stability at moderate and high lift coefficients. Since the particular configuration tested was not an optimum flat-fuselage design, however, these unsatisfactory characteristics were not considered to be necessarily indicative of the results that would be obtained with other flat-fuselage arrangements.

INTRODUCTION

Some recently proposed airplane designs have incorporated fuselages of relatively flat cross section with the major axis horizontal. A study made to determine the static stability characteristics of some flat-fuselage models (ref. 1) indicated that these models exhibit static lateral stability characteristics that are generally similar to those of a canard model (ref. 2); that is, at low angles of attack with vertical tails off, flat-fuselage models were directionally unstable, but at high angles of attack, the sidewash from the nose of the models caused an effective reversal in the direction of sideslip of the fuselage which resulted in the model being directionally stable. At high angles of attack, however, this sidewash also caused a reduction in the directional stability contributed by a vertical tail located at the rear of the fuselage. Free-oscillation tests (ref. 3) showed that, for the vertical-tail-off condition, the damping in yaw decreased and in some cases became negative when the static directional stability increased with increasing angle of attack. On the other hand, at high angles of attack, the vertical tail which decreased the static directional stability provided a large increase in the damping in yaw.

Because of the unusual nature of these lateral stability characteristics, an investigation was undertaken to flight-test a flat-fuselage model in the Langley free-flight tunnel in order to determine the effect of these characteristics on dynamic lateral stability and general flying qualities. The model in the basic condition had vertical tip tails installed since results of a previous investigation (ref. 3) had shown that this configuration produced satisfactory static stability characteristics. Flight tests were made with the model in the basic condition and also with a center vertical tail in combination with the tip tails. The various vertical-tail arrangements were studied with the leading-edge flaps both retracted and extended.

SYMBOLS

All forces and moments are referred to the stability axes originating at a center-of-gravity position of 0.025 mean aerodynamic chord ahead of the leading edge of the mean aerodynamic chord. A sketch showing the positive direction of the forces and moments is presented in figure 1.

The symbols and coefficients are defined as follows:

C_L lift coefficient, Lift/qS

C_D drag coefficient, Drag/qS

C_m pitching-moment coefficient, $M/qS\bar{c}$

C_Y lateral-force coefficient, Y/qS

C_l rolling-moment coefficient, L/qSb

C_n yawing-moment coefficient, N/qSb

L rolling moment, about X-axis

M	pitching moment, about Y-axis
N	yawing moment, about Z-axis
Y	lateral force, lb
q	dynamic pressure, $\frac{1}{2}\rho V^2$, lb/sq ft
S	wing area, sq ft
b	wing span, ft
c	wing chord, ft
$\bar{c}$	mean aerodynamic chord, $\frac{2}{S}\int_0^{b/2} c^2\,dy$, ft
ρ	mass density of air, slugs/cu ft
V	airspeed, ft/sec
β	angle of sideslip, deg
$\dot{\beta}$	sideslipping velocity, radians/sec
γ	glide-path angle, deg
δ_r	rudder deflection, deg
δ_a	aileron deflection perpendicular to hinge line (elevons deflected differentially for aileron control), deg
δ_e	elevator deflection perpendicular to hinge line (elevons deflected together for elevator control), deg
ψ	angle of yaw, deg
ϕ	angle of bank, deg
α	angle of attack, deg
$rb/2V$	yawing-angular-velocity parameter, radians
r	yawing angular velocity, radians/sec
I_X	rolling moment of inertia, slug-ft^2

I_Y pitching moment of inertia, slug-ft^2

I_Z yawing moment of inertia, slug-ft^2

$C_{Y_\beta} = \dfrac{\partial C_Y}{\partial \beta}$

$C_{n_\beta} = \dfrac{\partial C_n}{\partial \beta}$

$C_{l_\beta} = \dfrac{\partial C_l}{\partial \beta}$

$C_{n_r} = \dfrac{\partial C_n}{\partial \frac{rb}{2V}}$

$C_{n_{\dot{\beta}}} = \dfrac{\partial C_n}{\partial \frac{\dot{\beta} b}{2V}}$

APPARATUS AND MODEL

The investigation was made in the Langley free-flight tunnel which is designed to test free-flying dynamic models. A complete description of the tunnel and its operation is given in reference 4.

A three-view drawing of the model is presented in figure 2 and a photograph of the model with flaps retracted and tip tails on is presented in figure 3. Dimensional and mass characteristics of the model are given in table I.

The model was equipped with wing-tip tails in the basic condition. For some tests a center vertical tail was also installed at the rear of the fuselage. (See fig. 2.) Surfaces located at the trailing edge of the wing were deflected together to give elevator control or differentially to provide aileron control. Only the tip tails had rudder surfaces and they were deflected with the ailerons to give coordinated control. During a part of the investigation the rudder area was increased by about 33 percent by the addition of 1/2-inch balsa extensions to the trailing edge of the rudders. A leading-edge flap located on the outboard half of the wing (fig. 2) was used in some tests.

DETERMINATION OF THE STATIC STABILITY AND CONTROL AND DAMPING-IN-YAW CHARACTERISTICS OF THE FLIGHT-TEST MODEL

Force tests were made to determine the static longitudinal and lateral stability and control characteristics of the model over an angle-of-attack range from 0° to 40° with leading-edge flap retracted and extended and with tip tails on. The lateral characteristics were also determined with all tails off, with only the center tail on, and with the center vertical tail in combination with the tip tails. The lateral characteristics were determined from measurements of force and moment coefficients over the angle-of-attack range at $\pm 5^\circ$ sideslip and over a sideslip range of $\pm 20^\circ$ at angles of attack of 0°, 16°, 24°, 28°, and 32°. Most of the tests were made with the elevons deflected -15° or -20° which corresponded to those deflections required for trim in most of the flight tests. All force tests were made at a dynamic pressure of 3.0 pounds per square foot which corresponds to an airspeed of approximately 50 feet per second at standard sea-level conditions and to a test Reynolds number of about 4.4×10^5 based on the mean aerodynamic chord of 1.383 feet.

Free-oscillation tests to determine the damping-in-yaw characteristics were made over an angle-of-attack range from 0° to 32° with flaps retracted and extended and with tip tails off and on. Tests were also made at an angle of attack of 32° with only the center tail on. The tests were made at a dynamic pressure of 1.2 pounds per square foot which corresponds to an airspeed of approximately 31 feet per second and a test Reynolds number of 2.75×10^5 based on the mean aerodynamic chord.

Longitudinal Stability and Control Characteristics

The data presented in figure 4 show the effect of elevator deflection on the longitudinal stability and control characteristics of the model with flaps retracted. The data show that in general the stability was satisfactory from 0° to 16° and from 24° to near the stall. For all elevator settings the model had less stability in the angle-of-attack range from 16° to 24° and became unstable at the stall. The data also show that the elevator effectiveness decreases considerably at moderate lift coefficients as the deflection is increased from -20° to -30°.

These data show that, although the maximum lift of the model as measured in force tests is fairly high, it would be impossible to realize these values in the model flight tests because of the low stability at moderate angles of attack. The maximum trimmed lift coefficient that could be attained with the center-of-gravity position for which the data of figure 4 are presented ($0.025\bar{c}$ ahead of the mean aerodynamic chord) is about 0.5 (obtained with an elevon deflection of -30°). The maximum trimmed lift coefficient could be increased to 0.7 or 0.8 by moving the center of gravity slightly rearward from the position for which these data are presented and by using elevator deflections of about -10° or -20°.

A comparison is made in figure 5 of the longitudinal characteristics of the present model and those of the model of reference 5 which has a wing identical to that of the present model but which has a circular-cross-section fuselage with a maximum diameter of about 6 inches. The data show that the maximum lift coefficient of the flat-fuselage model is about 0.55 greater than that of the circular-fuselage model. It would appear from the data of reference 1 that only a portion of this increase in lift coefficient may be attributed to the greater lift of the flat fuselage compared with that of the circular fuselage; therefore, the remainder of the lift must result from the effect of the fuselage on the flow over the wing. The flow surveys of figure 6 indicate that the flat fuselage continues to produce lift even at angles of attack above that at which the wing begins to stall. These surveys show that the outboard portion of the wing is stalled at an angle of attack of 16° whereas the flow over the fuselage is, for the most part, unstalled up to an angle of attack of at least 32°.

The data of figure 5 also show that the two models had about the same static longitudinal stability characteristics at low lift coefficients. At high lift coefficients, however, the circular-fuselage model became more stable whereas the flat-fuselage model became less stable and eventually became unstable at the stall. The increased lift of the flat fuselage, particularly at high angles of attack, would tend to produce a nose-up pitching moment and reduce the static stability of the model. (See ref. 1.)

The data of figure 7 show the effect of the leading-edge flap on the longitudinal characteristics of the model with -20° elevator deflection. As can be seen, the flap had relatively little effect on the maximum lift coefficient, but it did reduce the drag by cleaning up the flow at the wing tip. Extending the flap had little effect on the longitudinal stability.

Lateral Stability and Control Characteristics

The data of figure 8 show the effect of vertical-tail arrangement on the lateral stability characteristics of the model at various angles of attack. Summarized in figure 9 are the yawing-moment data of figure 8 in terms of the directional stability parameter C_{n_β} as measured at low ($\beta < \pm 5^{\circ}$) and high ($\beta > \pm 5^{\circ}$) angles of sideslip for each tail configuration. These data show that, up to 16° angle of attack, there is little difference in the values of $C_{n_{\beta}}$ measured at low or high angles of sideslip. At 24° angle of attack, however, the values of $C_{n_{\beta}}$ measured at low angles of sideslip are generally higher than those measured at high sideslip angles. Above this angle of attack, $C_{n_{\beta}}$, measured at low sideslip angles, decreases sharply and generally becomes less than that measured at high sideslip angles. With all tails off or center tail on, $C_{n_{\beta}}$ becomes greatly negative at 32° angle of attack.

Adding tip or center vertical tails generally increased the directional stability of the model with the center tail being more effective than the tip tails over the low and moderate lift coefficient range. In the high angle-of-attack range, however, the effectiveness of the center tail decreased so that the directional stability of the model with either center tail alone or center plus tip tails became less than that of the model with only tip tails. The angle of attack at which the effectiveness of the center tail decreased varied with sideslip angle, but the results were generally similar for both low and high angles of sideslip.

The data of figure 10 show that extending the leading-edge flap had relatively little effect on the directional stability $C_{n_{\beta}}$ at low and moderate angles of attack but increased $C_{n_{\beta}}$ appreciably in the high angle-of-attack range. The flap also increased the effective dihedral $-C_{l_{\beta}}$ at moderate and high angles of attack.

The variation of aileron and rudder effectiveness with angle of attack is presented in figure 11. The rolling moment produced by aileron deflections of $\pm 20^{\circ}$ from a neutral setting of -15° decreases by about 40 percent as the angle of attack is increased from low to moderate values. Further increases in the angle of attack resulted in the rolling effectiveness increasing slightly. The yawing moment produced by the ailerons is adverse over the entire angle-of-attack range and becomes more adverse as the angle of attack increases. The yawing moment produced by a rudder deflection of 10° decreases very rapidly with increasing angle of attack and reaches a minimum at about 16° angle of attack. Up to 8° angle of attack, the yawing moment produced by the rudder is sufficiently large to balance the adverse yawing moment produced by $\pm 20^{\circ}$ deflection of the ailerons. Increasing the rudder area by 33 percent increased the rudder effectiveness by about 20 to 40 percent.

Damping-in-Yaw Characteristics

The data of figure 12 are the damping-in-yaw characteristics of the model as presented in reference 3. The damping characteristics with all tails off were generally the same with flaps both retracted and extended except at high angles of attack where the increase in drag associated with wing-tip stall caused a large increase in the damping of the model with flaps retracted. With tip tails on, the damping was slightly greater with flaps extended except at high angles of attack where the damping became negative. The addition of a center vertical tail produced a large positive increment of damping at high angles of attack.

FLIGHT TESTS

Flight tests were made to determine the flying characteristics of the model over a lift-coefficient range from 0.35 to 0.80. Control was obtained by simultaneous deflection of the ailerons and rudder. The aileron deflections varied from $\pm 12^{\circ}$ to $\pm 30^{\circ}$ with the largest deflections being used at the highest lift coefficients. An effort was made to trim out the adverse yawing moment produced by the ailerons whenever possible by using rudder deflections up to a maximum of 10° and in some cases increasing the rudder area by 33 percent. The behavior of the model during flights in which the ailerons alone were used for lateral control was also studied. Flights were made with tip tails and with both tip and center tails for the flap-retracted and flap-extended conditions. Most of the flights were made with the center of gravity located at 0.025 mean aerodynamic chord ahead of the leading edge of the mean aerodynamic chord. A few flights were also made with the center of gravity moved forward 0.05 mean aerodynamic chord. Motion pictures of the tests were taken to supplement the pilot's observation of the over-all behavior of the model.

RESULTS AND DISCUSSION

In this investigation it was possible to study the dynamic stability and control characteristics of the model over a lift-coefficient range from only 0.35 to 0.80 because of various limiting factors. The minimum lift coefficient was, of course, determined by the maximum tunnel velocity and wing loading of the model. The maximum trimmed lift coefficient obtained in the flight tests was very low compared to the maximum lift coefficient measured in force tests because of the limitations imposed on the maximum trimmed lift coefficient by the static longitudinal stability characteristics as pointed out in the discussion of force-test results.

Longitudinal Stability and Control Characteristics

The dynamic longitudinal stability and control characteristics of the model with leading-edge flaps both retracted and extended were generally satisfactory at the lower lift coefficients tested. The model flew smoothly and the response to elevator deflection appeared to be satisfactory. As the lift coefficient increased, however, the behavior of the model became somewhat erratic and the model was more difficult to control. At the highest lift coefficients at which flights were attempted (about 0.8 lift coefficient and 20° angle of attack), the model exhibited a nosing-up tendency. This result is explained by the data of figure 4 which show that, at lift coefficients around 0.8, the model has very low static stability or instability, depending upon the elevator deflection. The low static stability caused longitudinal unsteadiness because of the increased response of the model to control or gust disturbances. Flights made with the center of gravity moved forward about $0.05\bar{c}$ to increase the static stability showed some improvement in the longitudinal characteristics. For these conditions, however, the maximum trimmed lift coefficient obtainable was reduced. The lift-coefficient range that could be studied in the present investigation was, therefore, seriously limited because of the inability to attain a longitudinally stable condition in the higher angle-of-attack range.

In addition to the unsteadiness resulting from low static longitudinal stability, some of the erratic behavior in pitch was apparently caused by random changes in trim. These random trim changes were probably caused by irregular fluctuations in the vortex flow produced by the forward portion of the fuselage. The flow behind the nose of a flat-fuselage model is believed to be similar to the flow behind a canard surface. The results of reference 6, which show the flow field behind a canard surface, will, therefore, serve to illustrate the changes in flow that are probably responsible for the random trim changes. These results show rather large variations in the asymmetrical disposition of the vortices as a result of relatively small changes in sideslip and angle of attack. Because of the constantly changing attitude of the model resulting from the unsteadiness associated with the low static longitudinal stability (and the low dynamic lateral stability, which will be discussed later), the fluctuations in the flow over the wing are probably rather large and add further to the over-all erratic behavior of the model.

Another factor which influenced the longitudinal behavior of the model and contributed to the pilot's poor opinion of the over-all flight characteristics at the higher lift coefficients was the large variation of drag with lift, which is generally a characteristic of low-aspect-ratio swept wings (ref. 7). This large variation of drag with lift caused large variations of glide angle with lift coefficient since the trim glide angle is a function of the drag-lift ratio (fig. 13).

The over-all longitudinal flight characteristics were considered to be generally unsatisfactory for most of the conditions tested. Although it was impossible to cover the entire lift range, an analysis of the force tests indicates that the model would have a rather severe nosing-up tendency near the stall (fig. 4) and that the difficulty associated with the random trim changes and with the large variation of drag with lift would become even more troublesome at lift coefficients above those attained in the flight tests.

Lateral Stability and Control Characteristics

The lateral stability and control characteristics of the model were fairly satisfactory at low lift coefficients $\left(C_L \cong 0.35\right)$ but were definitely unsatisfactory at the highest lift coefficients flown $\left(C_L \cong 0.80\right)$ regardless of flap or vertical-tail configuration because of low oscillatory stability and poor aileron control characteristics. Extending the flap caused the oscillatory stability and over-all flying characteristics to be slightly worse than those with flaps retracted. Because of the similarity of results obtained with flaps retracted or extended, no attempt has been made in the following discussion to distinguish between the flap retracted or extended configurations.

Effect of vertical-tail configuration.- The lateral oscillation was fairly well damped at low lift coefficients with the tip tails on, but the damping of the lateral oscillation decreased as the lift coefficient increased, until at the highest lift coefficients tested, the model appeared to have approximately neutral oscillatory stability. It was difficult to obtain smooth flights at high lift coefficients because of this low oscillatory stability. Also contributing to the poor flight characteristics were the fluctuations in the vortex flow previously discussed. The large changes in vortex disposition with angle of sideslip which resulted in changes in damping in yaw and static lateral stability also appeared to cause random trim changes in yaw. At times the model would yaw and stay trimmed at some angle of sideslip for a short time and then perhaps change its angle of sideslip or slide into the tunnel wall. At other times the behavior of the model following a disturbance was characterized by large-amplitude rolling and yawing motions which made it necessary for the pilot to continually control the model in an effort to maintain flight. If the pilot did not effect recovery during the first two or three oscillations, the model usually sideslipped across the tunnel and crashed into the wall.

With the addition of the center vertical tail it appeared that the damping of the lateral oscillation was increased but the oscillatory stability was still unsatisfactory at the higher lift coefficients. At low lift coefficients with the center vertical tail, it appeared to the pilot that the model had increased damping in roll. In this case the increase in oscillatory stability brought about by increased directional stability (fig. 9) and increased damping in yaw (fig. 12) probably gave the impression that the damping in roll was increased.

It was not possible to evaluate the effect of the decrease in directional stability produced by the center tail at high angles of attack because, as pointed out previously, the longitudinal stability and trim difficulties prevented flight tests from being made at high angles of attack.

Effect of aileron and rudder deflections.- It was found in the tests that aileron deflections of the order of $\pm 15^{\circ}$ gave about the best overall flight characteristics at the lower lift coefficients where coordinated aileron and rudder control was possible. This amount of control resulted in reasonably smooth flights and appeared to be sufficient to effect recovery after fairly large disturbances. At higher lift coefficients, however, larger control deflections were required with both tail configurations because of the decrease in aileron effectiveness and oscillatory stability. These large control deflections, which were needed to effect recoveries from the large angles of roll and yaw which the model reached after disturbances, also contributed to the erratic behavior of the model at times by causing the pilot to over-control when attempting to steady the model. One reason for the increased difficulty in flying the model with the large aileron deflections was the fact that the rudders were incapable of trimming out the adverse yawing moment produced by large aileron deflections because of the decrease in rudder effectiveness at high angles of attack (fig. 11(b)). This reduction in rudder effectiveness was evidenced in flight tests by increased yawing motions with increasing angle of attack.

When ailerons alone were used at the lowest lift coefficients flown (where the adverse yawing moments produced by the ailerons were at a minimum), reasonably good flight behavior was obtained although slight yawing motions were produced by the ailerons. As the lift coefficient increased, it became increasingly difficult to maintain flight, until, at the highest lift coefficients, the disturbing effect of the aileron yawing moments was so great that flight was impossible.

CONCLUDING REMARKS

An experimental investigation in the Langley free-flight tunnel to determine the dynamic stability and control characteristics of a model having a relatively flat fuselage with the major axis horizontal showed that, in flight, the model had an erratic behavior in pitch and yaw, apparently because of random trim changes associated with the flow from the forward portion of the flat fuselage. The model had an unusually high maximum lift coefficient because of its flat-fuselage design, but the maximum lift coefficient that could be obtained in flight tests was limited because of low dynamic lateral stability and low static longitudinal stability at moderate and high lift coefficients. Since the particular configuration tested was not an optimum flat-fuselage design, however, these unsatisfactory characteristics were not considered to be necessarily indicative of the results that would be obtained with other flat-fuselage arrangements.

Langley Aeronautical Laboratory,
National Advisory Committee for Aeronautics,
Langley Field, Va.

REFERENCES

1. Bates, William R.: Static Stability of Fuselages Having a Relatively Flat Cross Section. NACA RM L9I06a, 1949.

2. Draper, John W.: Low-Speed Static Stability Characteristics of a Canard Model With a 45° Sweptback Wing and a 60° Triangular Horizontal Control Surface. NACA RM L50G11, 1950.

3. Johnson, Joseph L.: Damping in Yaw and Static Directional Stability of a Canard Airplane Model and of Several Models Having Fuselages of Relatively Flat Cross Section. NACA RM L50H30a, 1950.

4. Shortal, Joseph A., and Osterhout, Clayton J.: Preliminary Stability and Control Tests in the NACA Free-Flight Wind Tunnel and Correlation With Full-Scale Flight Tests. NACA TN 810, 1941.

5. Johnson, Joseph L., Jr.: A Study of the Use of Various High-Lift Devices on the Horizontal Tail of a Canard Airplane Model As a Means of Increasing the Allowable Center-of-Gravity Travel. NACA RM L52K18a, 1953.

6. Johnson, Joseph L., Jr.: A Study of the Flow Field Behind the Triangular Horizontal Tail of a Canard Airplane at Approximately the Vertical-Tail Location by Means of a Tuft Grid. NACA RM L52H11, 1952.

7. McKinney, Marion O., Jr., and Drake, Hubert M.: Flight Characteristics at Low Speed of Delta-Wing Models. NACA RM L7K07, 1948.

TABLE I.- DIMENSIONAL AND MASS CHARACTERISTICS OF MODEL

Weight, lb	14.25
Wing loading, lb/sq ft, W/S	2.67
Mass density factor, μ	8.75
Moments of inertia:	
I_X, slug-ft^2	0.27
I_Y, slug-ft^2	0.84
I_Z, slug-ft^2	1.10
Wing:	
Airfoil section	NACA 0012
Area, sq ft	5.33
Span, ft	4.0
Sweepback of leading edge, deg	45
Aspect ratio	3.0
Incidence, deg	0
Dihedral, deg	0
Root chord, ft	1.77
Taper ratio	0.5
Mean aerodynamic chord, ft	1.383
Aileron area, sq ft (two ailerons)	0.84
Tip tails:	
Airfoil section	NACA 0009
Area, sq ft (two tails)	0.533
Span, ft	0.63
Sweepback of leading edge, deg	45
Root chord, ft	0.562
Taper ratio	0.50
Aspect ratio	1.49
Rudder area, percent tail area	30.00
Tail length, ft (center of gravity to leading edge of tip-tail root chord)	1.46
Center tail:	
Airfoil section	NACA 0009
Area, sq ft (measured above fuselage)	0.272
Span, ft (measured above fuselage)	0.73
Root chord, ft	0.495
Taper ratio	0.505
Aspect ratio	1.96
Tail length, ft (center of gravity to leading edge of center-tail root chord)	1.46

NACA

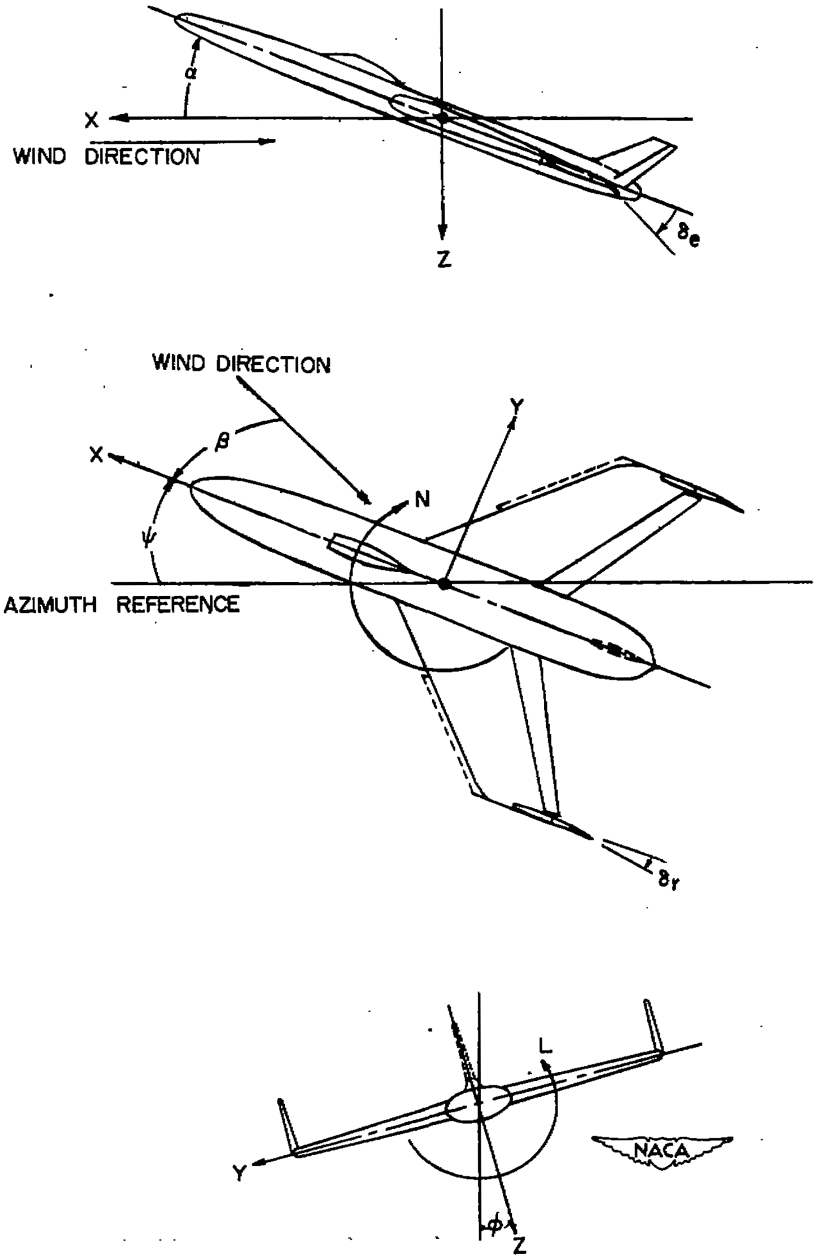

Figure 1.- The stability system of axes. Arrows indicate positive directions of moments, forces, and angles. This system of axes is defined as an orthogonal system having the origin at the center of gravity and in which the Z-axis is in the plane of symmetry and perpendicular to the relative wind, the X-axis is in the plane of symmetry and perpendicular to the Z-axis, and the Y-axis is perpendicular to the plane of symmetry. At a constant angle of attack, these axes are fixed in the airplane.

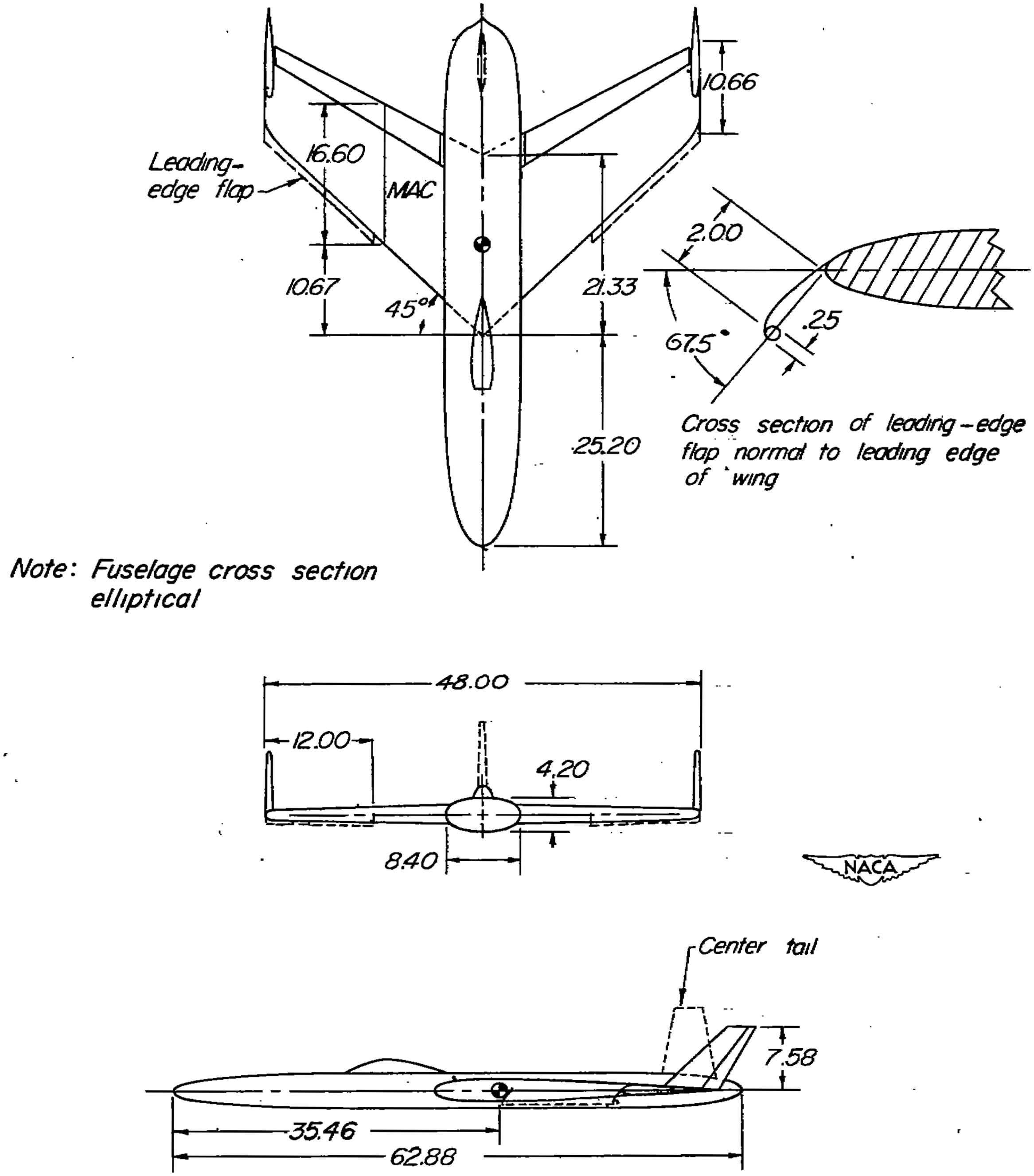

Figure 2.- Three-view drawing of model tested in the Langley free-flight tunnel. All dimensions are in inches.

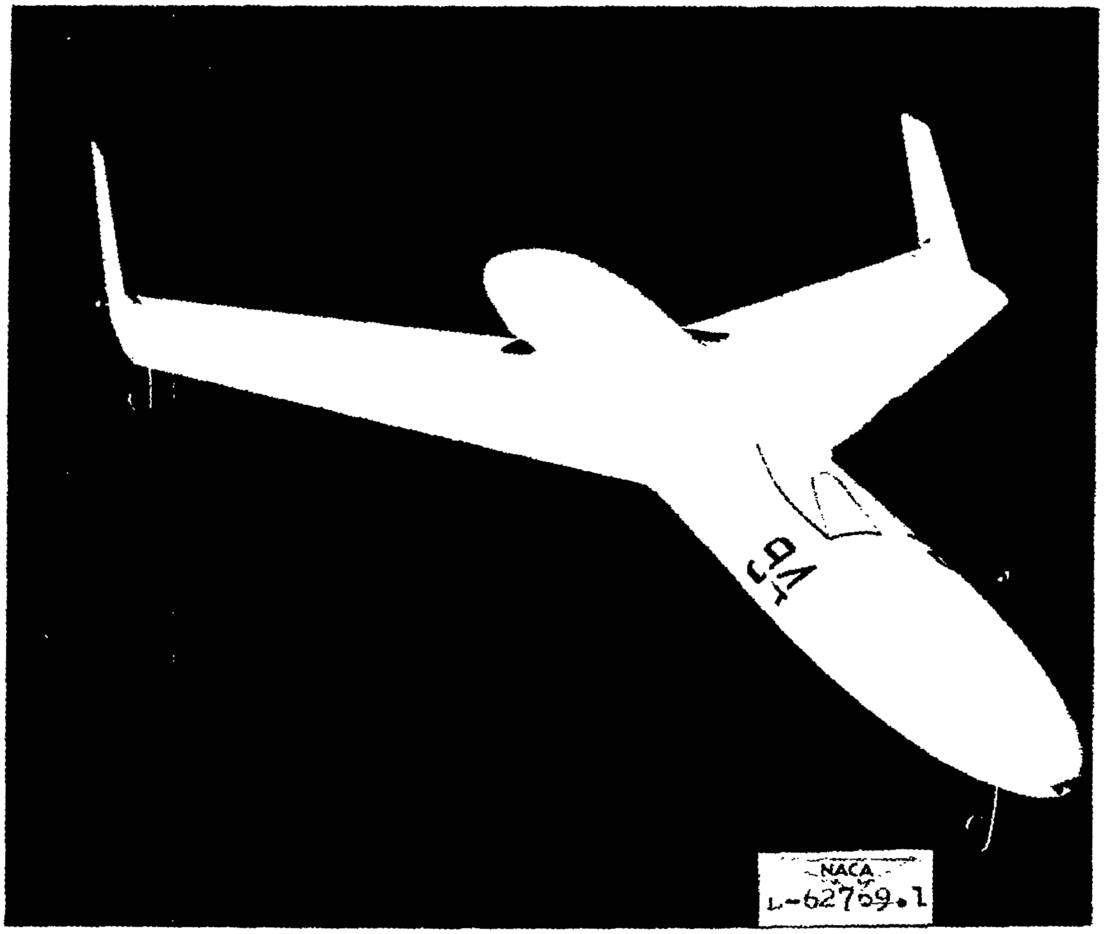

Figure 3.- Model tested in the Langley free-flight tunnel.

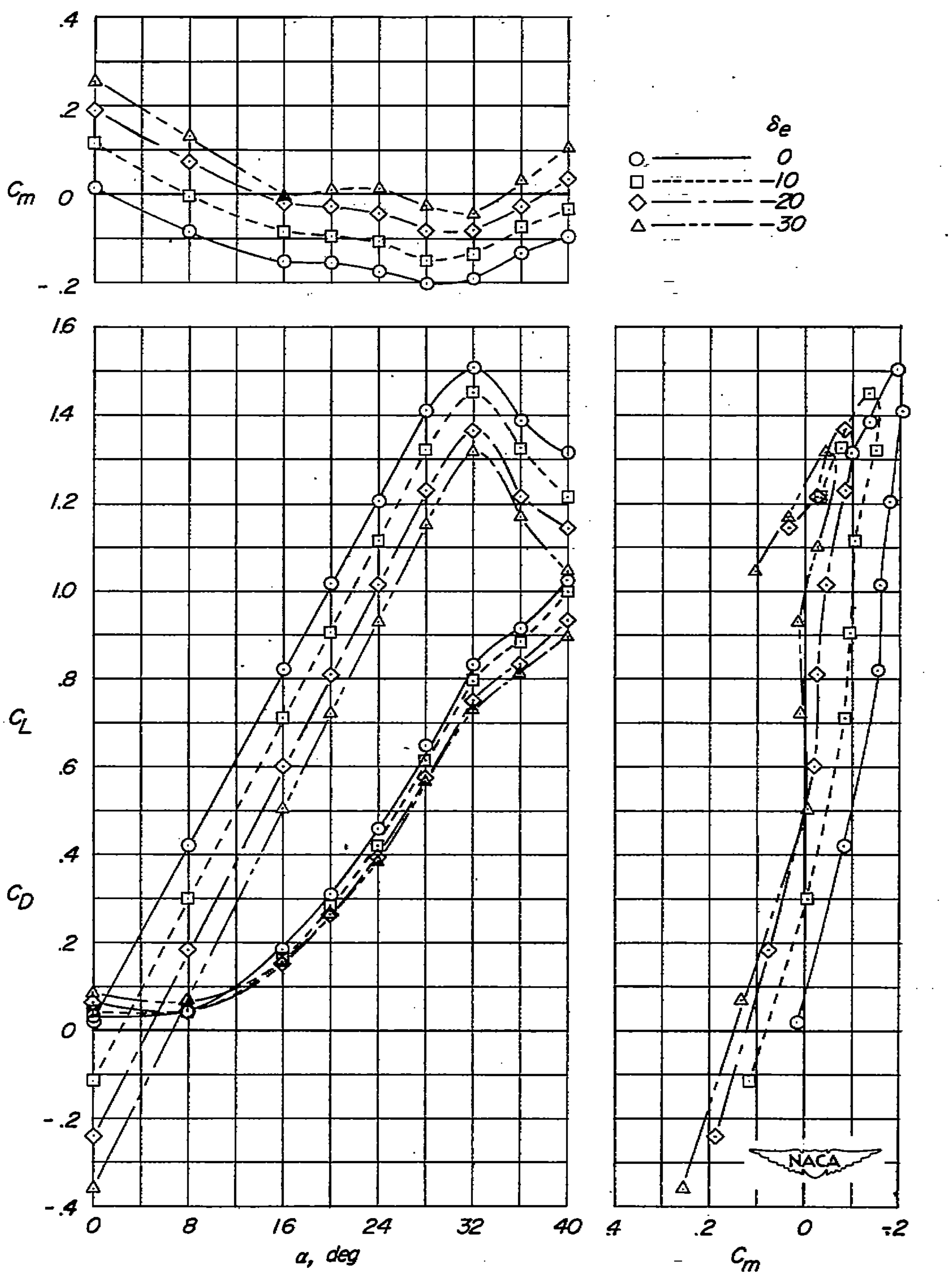

Figure 4.- Longitudinal stability and control characteristics of the model. Flap retracted; $\beta = 0^{\circ}$.

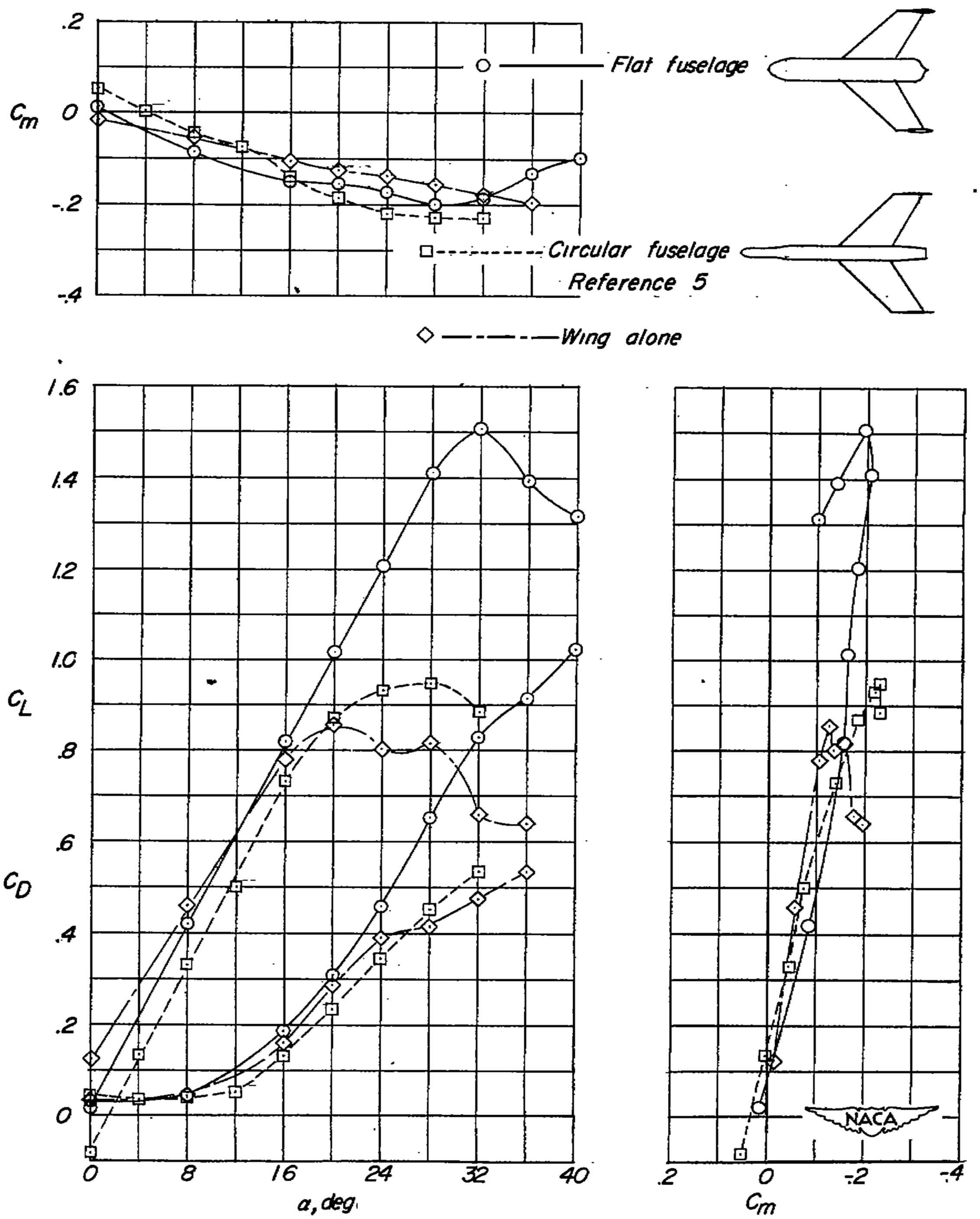

Figure 5.- Comparison of longitudinal characteristics of flat- and circular-fuselage models having identical wings. Flap retracted; $\delta_e = 0^{\circ}$; $\beta = 0^{\circ}$.

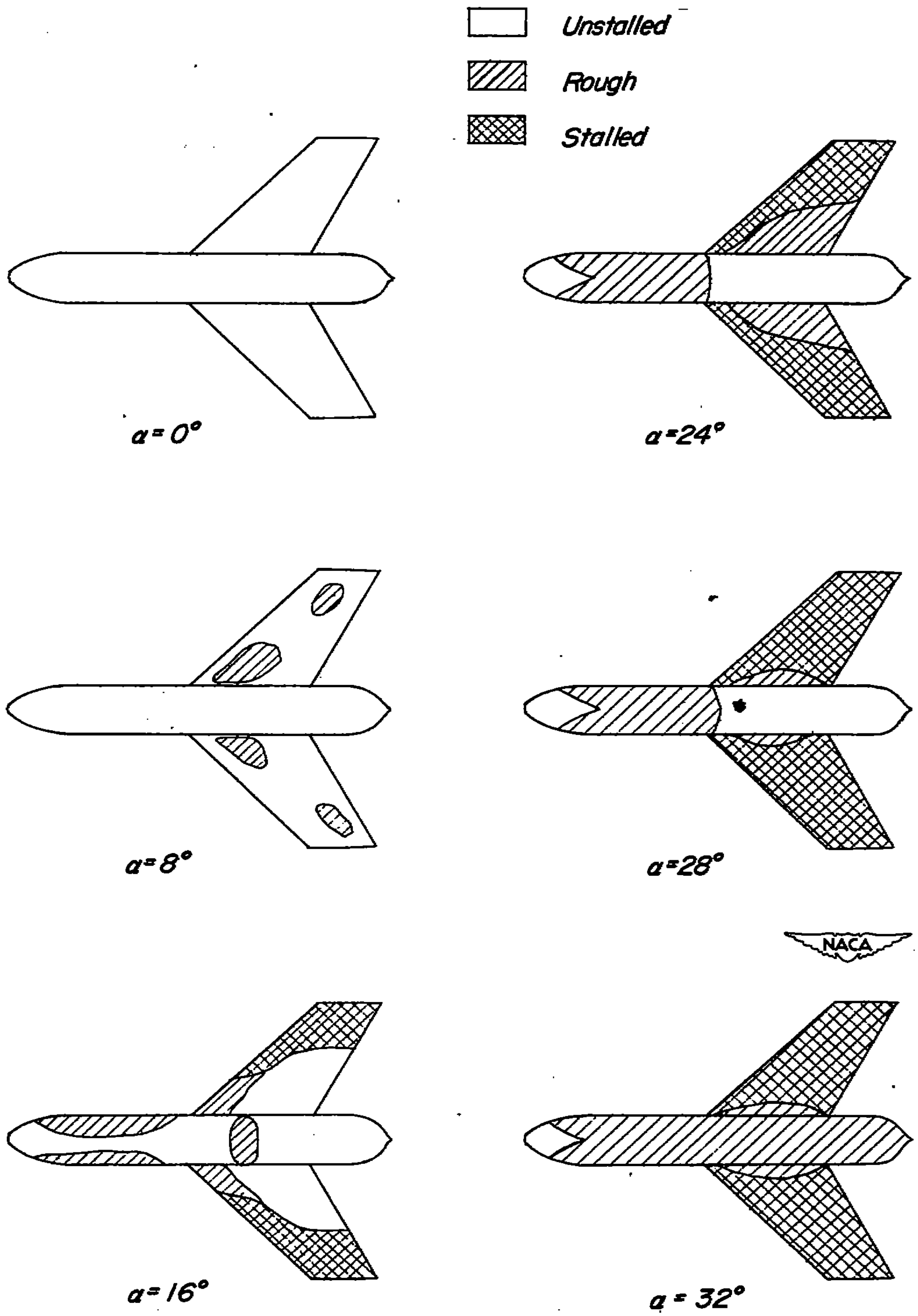

Figure 6.- Flow surveys of model. Flap retracted; tip tails off; $\delta_e = 0^\circ$; $\beta = 0^\circ$.

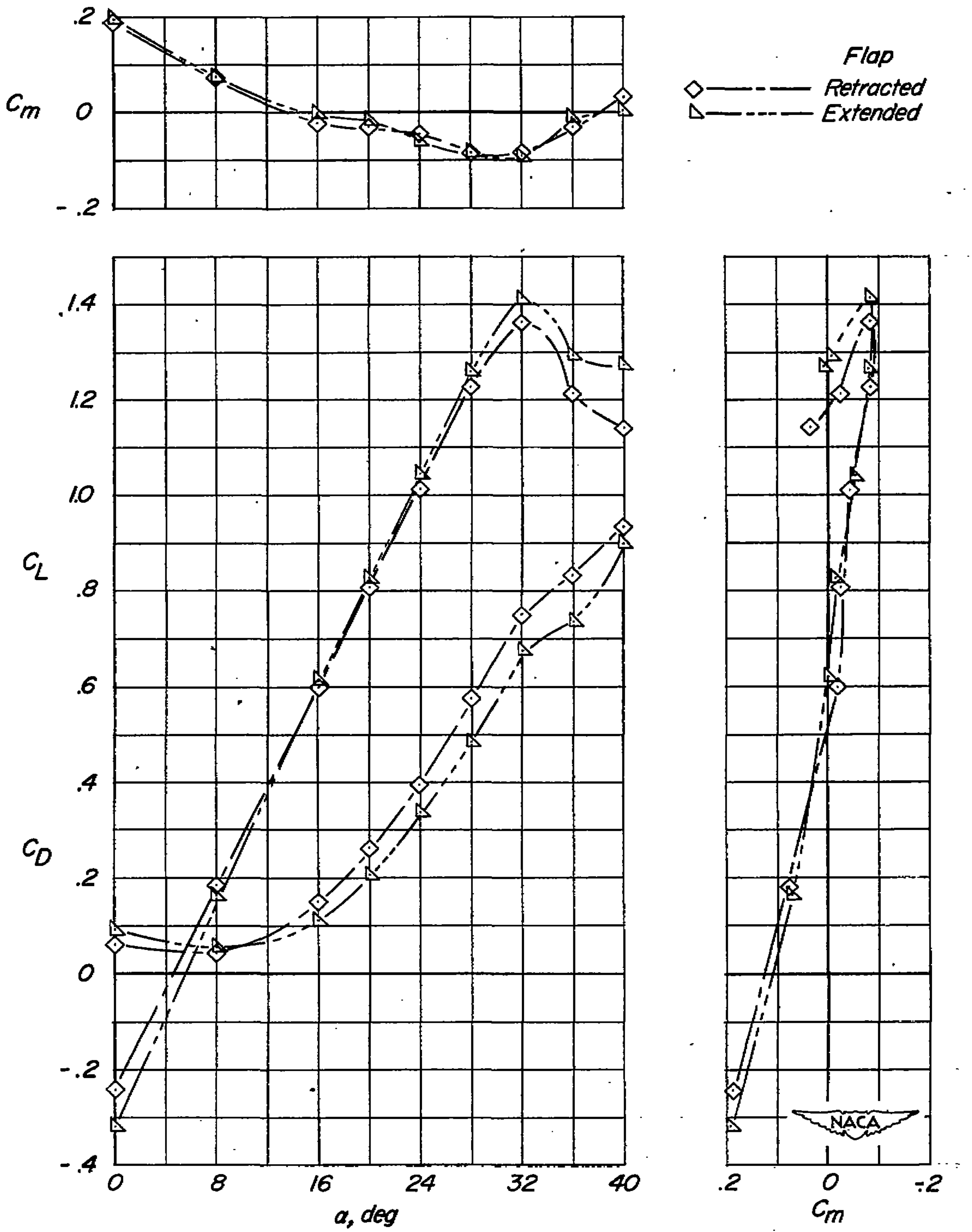

Figure 7.- Effect of leading-edge flap on longitudinal characteristics of model. $\delta_e = -20^\circ$; $\beta = 0^\circ$.

[redacted]

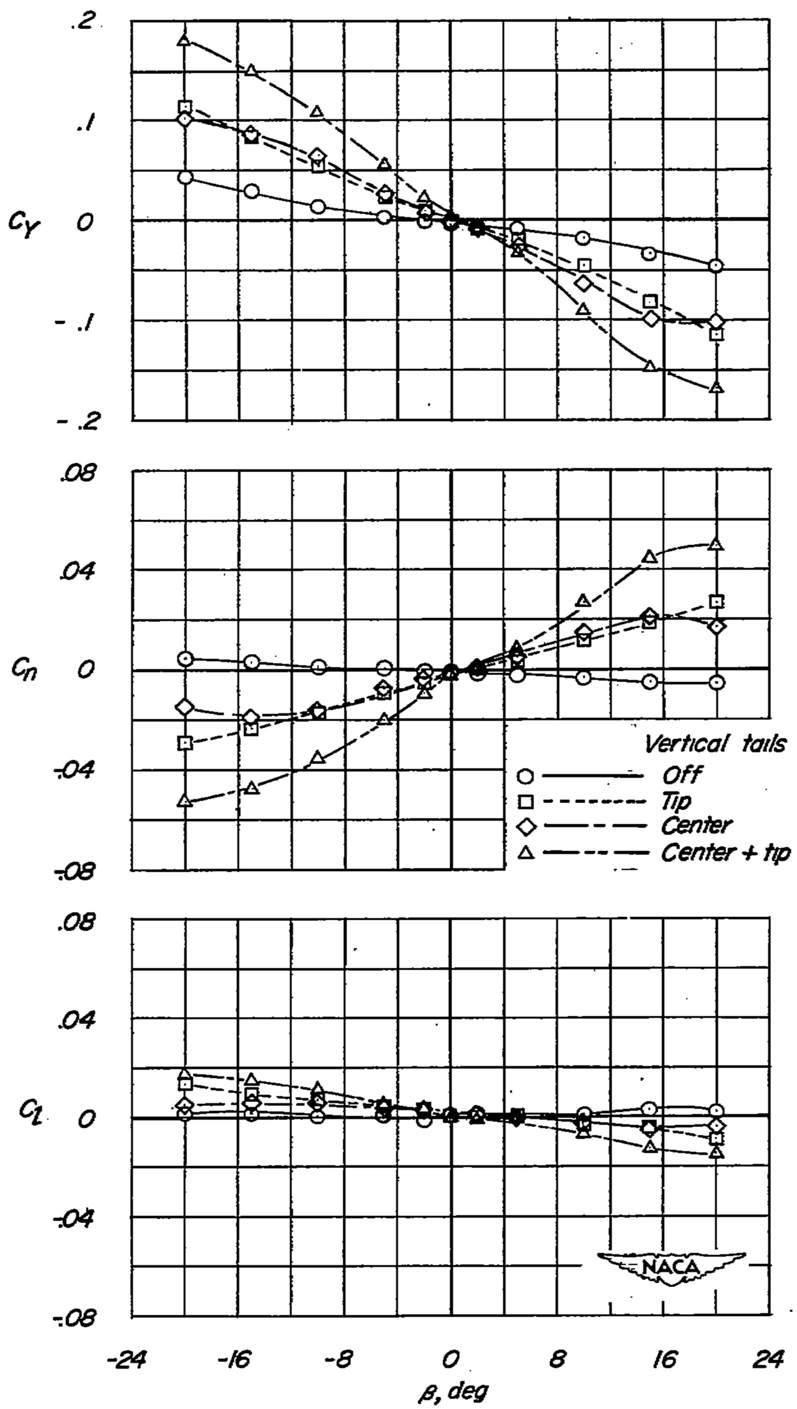

(a) $\alpha = 0°$.

Figure 8.- Lateral stability characteristics of model. Flap retracted; $\delta_e = -15^\circ$.

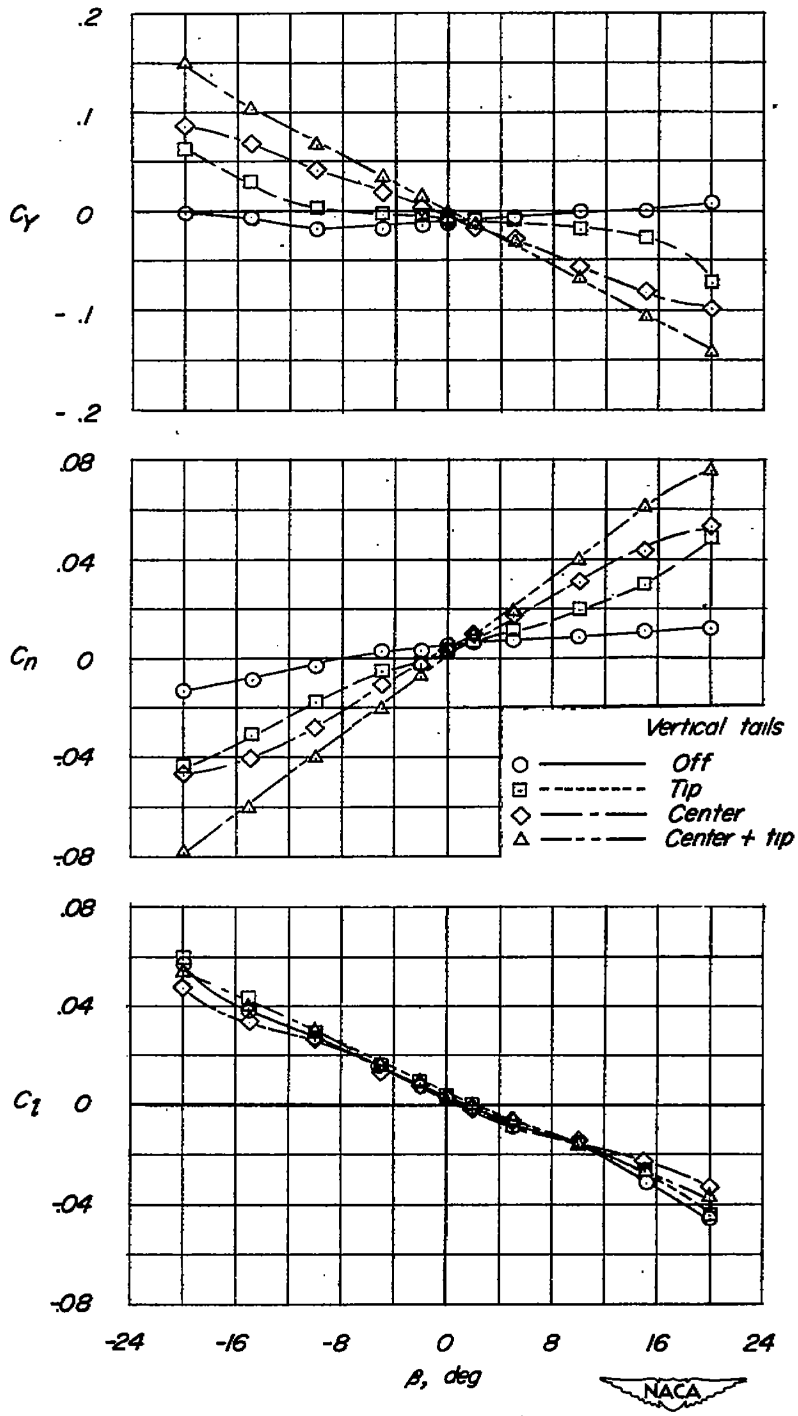

(b) $\alpha = 16°$.

Figure 8.- Continued.

[redacted]

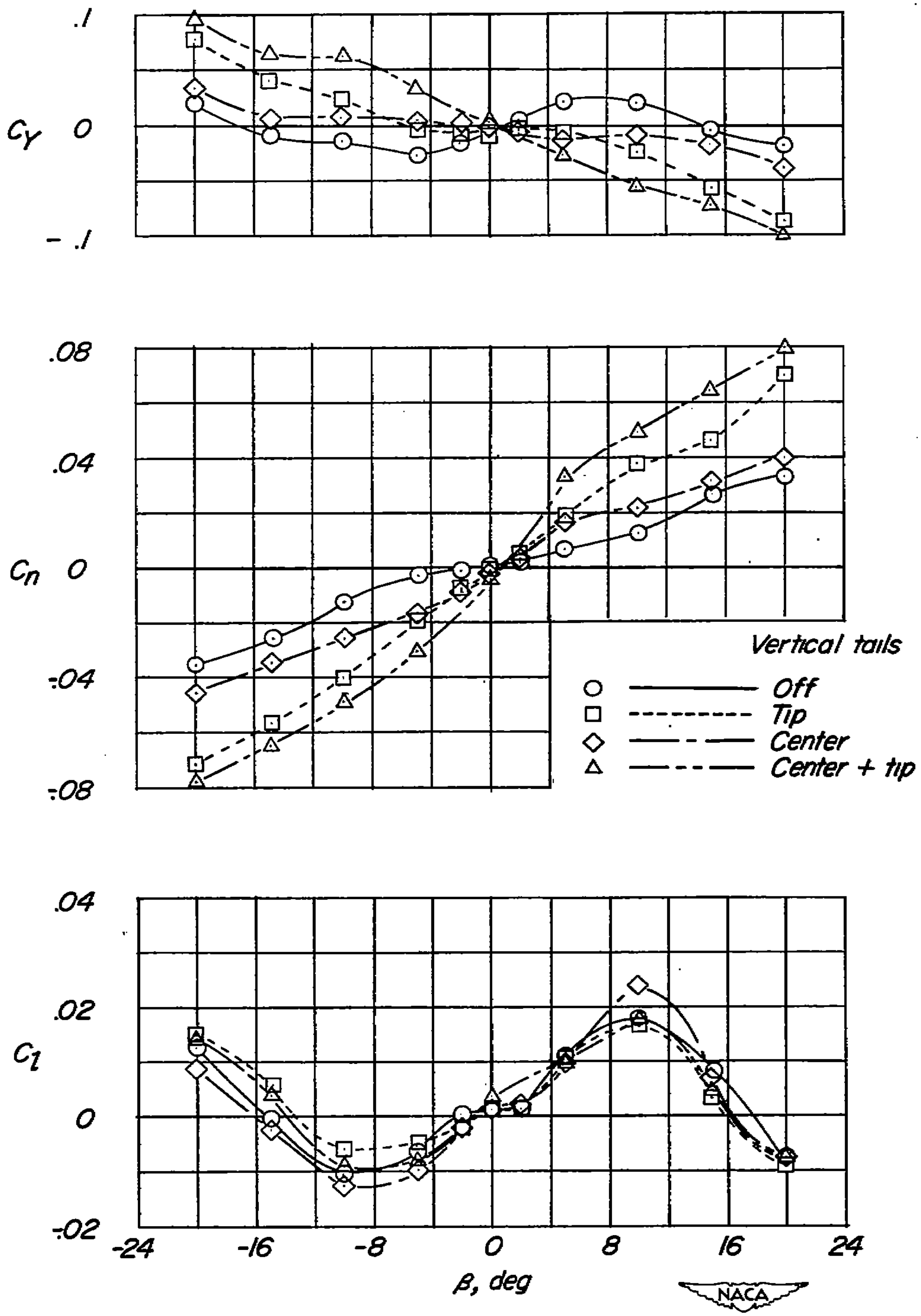

(c) $\alpha = 24°$.

Figure 8.- Continued.

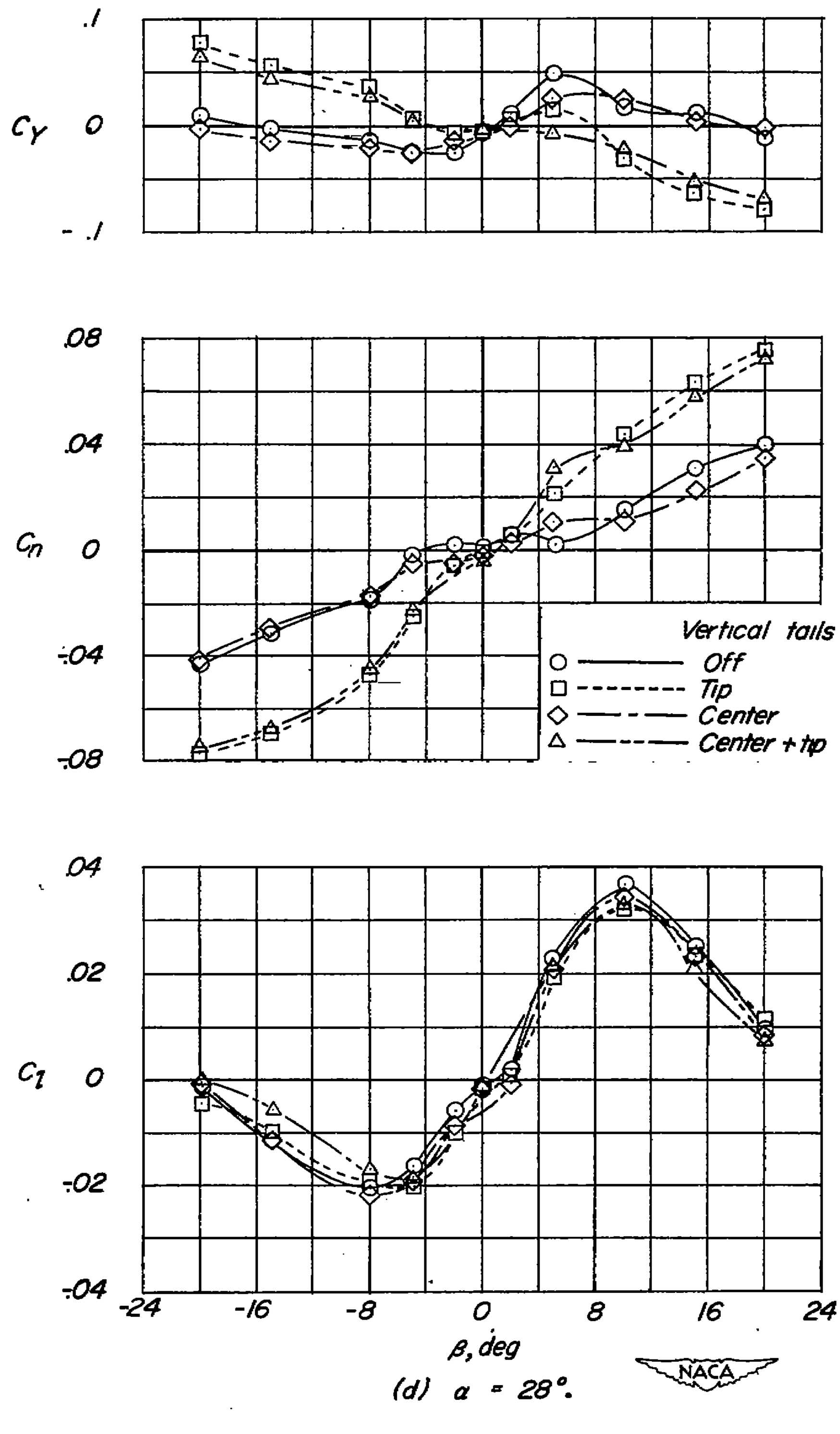

(d) $\alpha = 28°$.

Figure 8.- Continued.

[redacted]

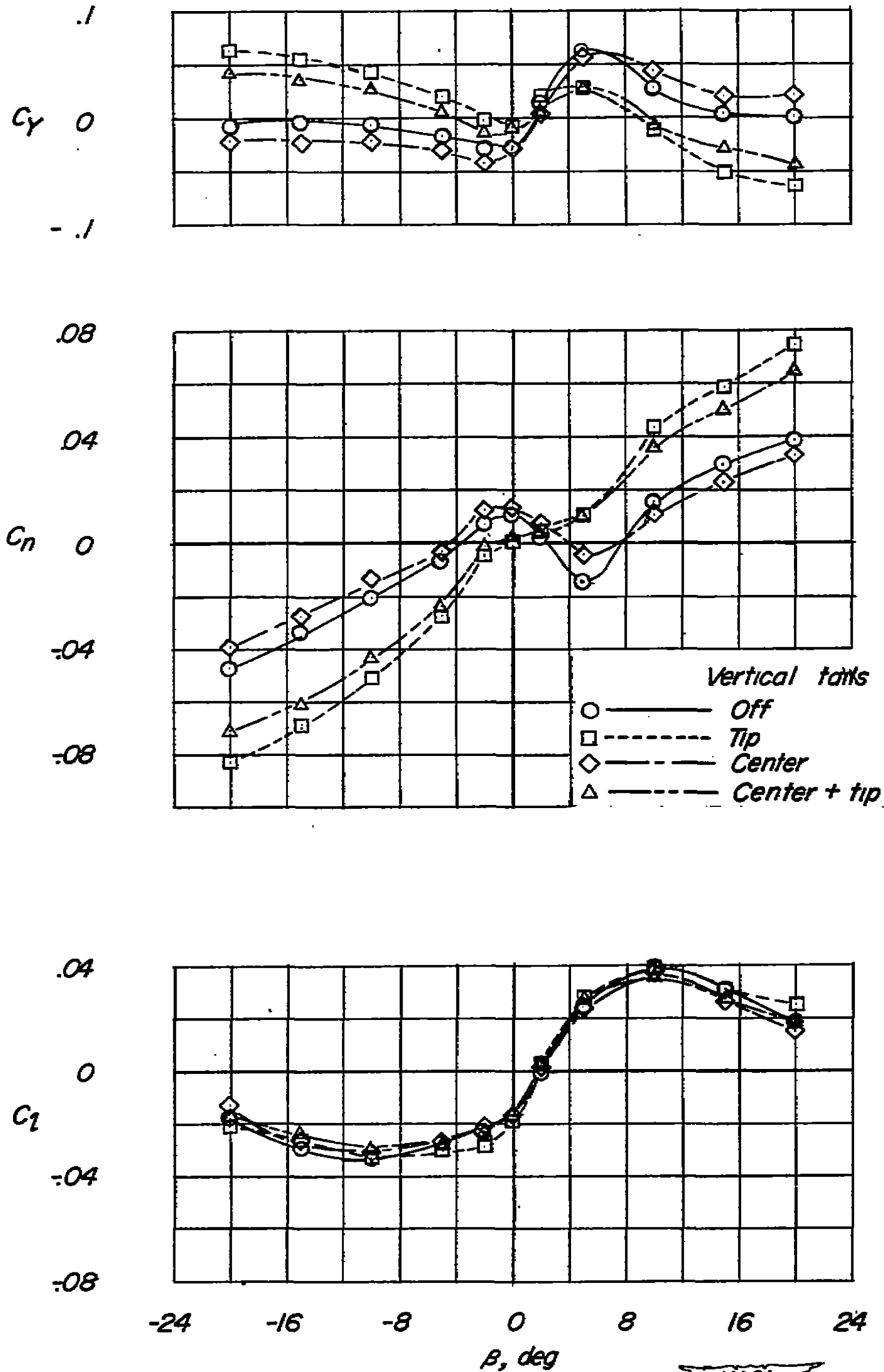

(e) $\alpha = 32°$.

Figure 8.- Concluded.

[redacted]

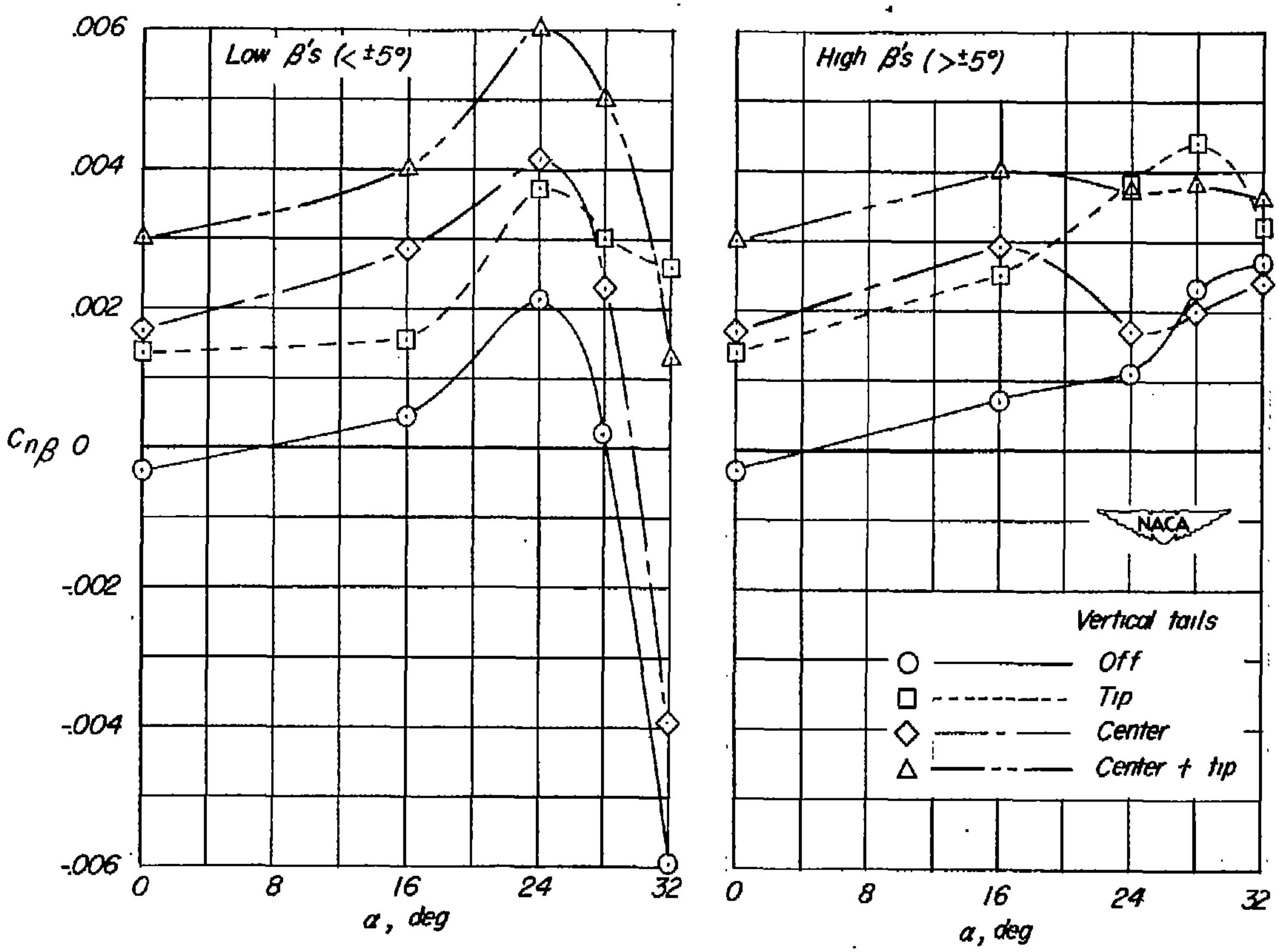

Figure 9.- Effect of vertical-tail configuration on directional-stability parameter C_{n_β} as measured at low and high angles of sideslip. Flaps retracted; $\delta_e = -15^\circ$.

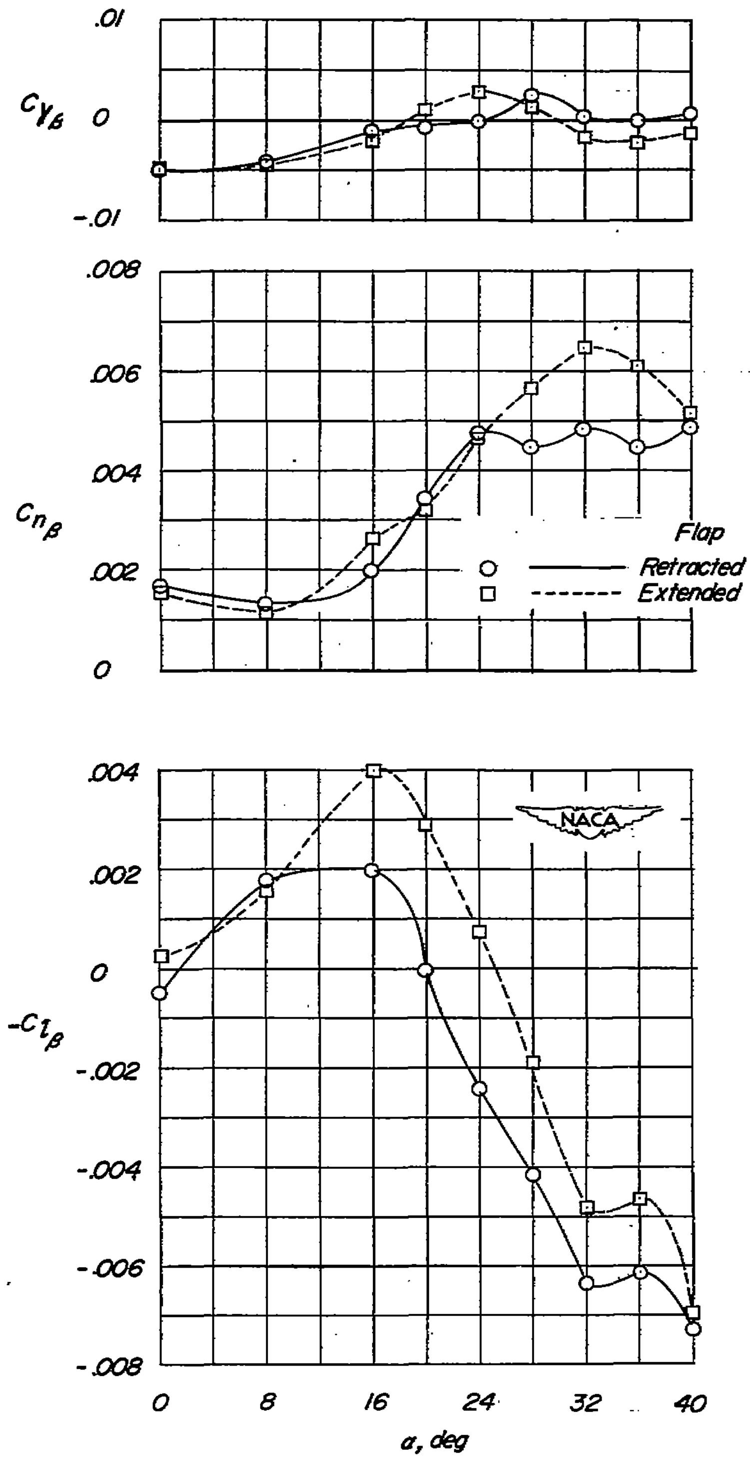

Figure 10.- Effect of leading-edge flap on lateral stability characteristics of model. $\delta_e = -20^\circ$; $\beta = \pm 5^\circ$.

[redacted]

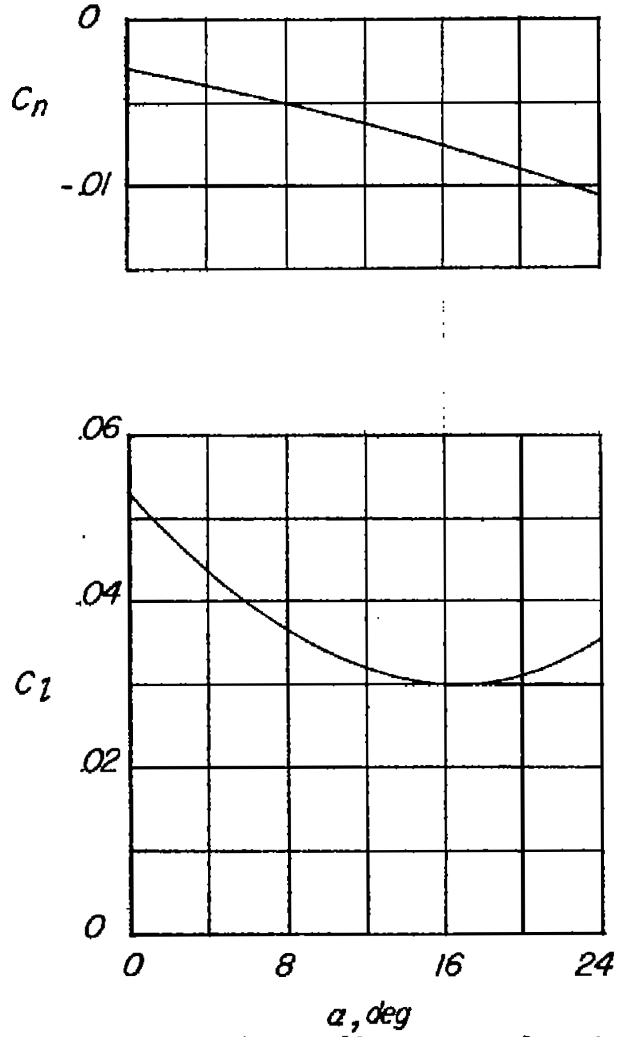

(a) Aileron effectiveness. $\delta_a = \pm 20°$.

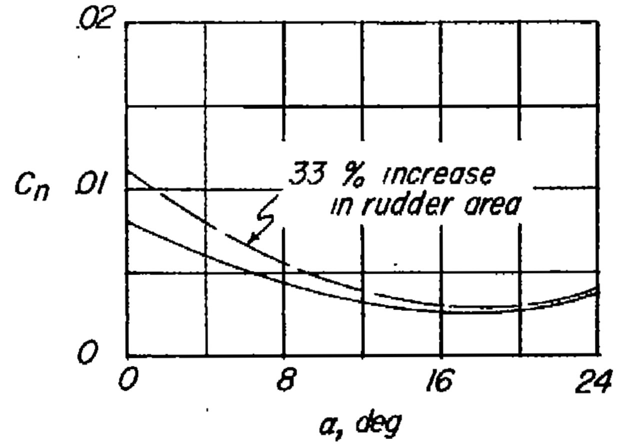

(b) Rudder effectiveness. $\delta_r = -10°$.

[redacted]

Figure 11.- Control characteristics of model. Flap retracted; $\delta_e = -15^{\circ}$.

[redacted]

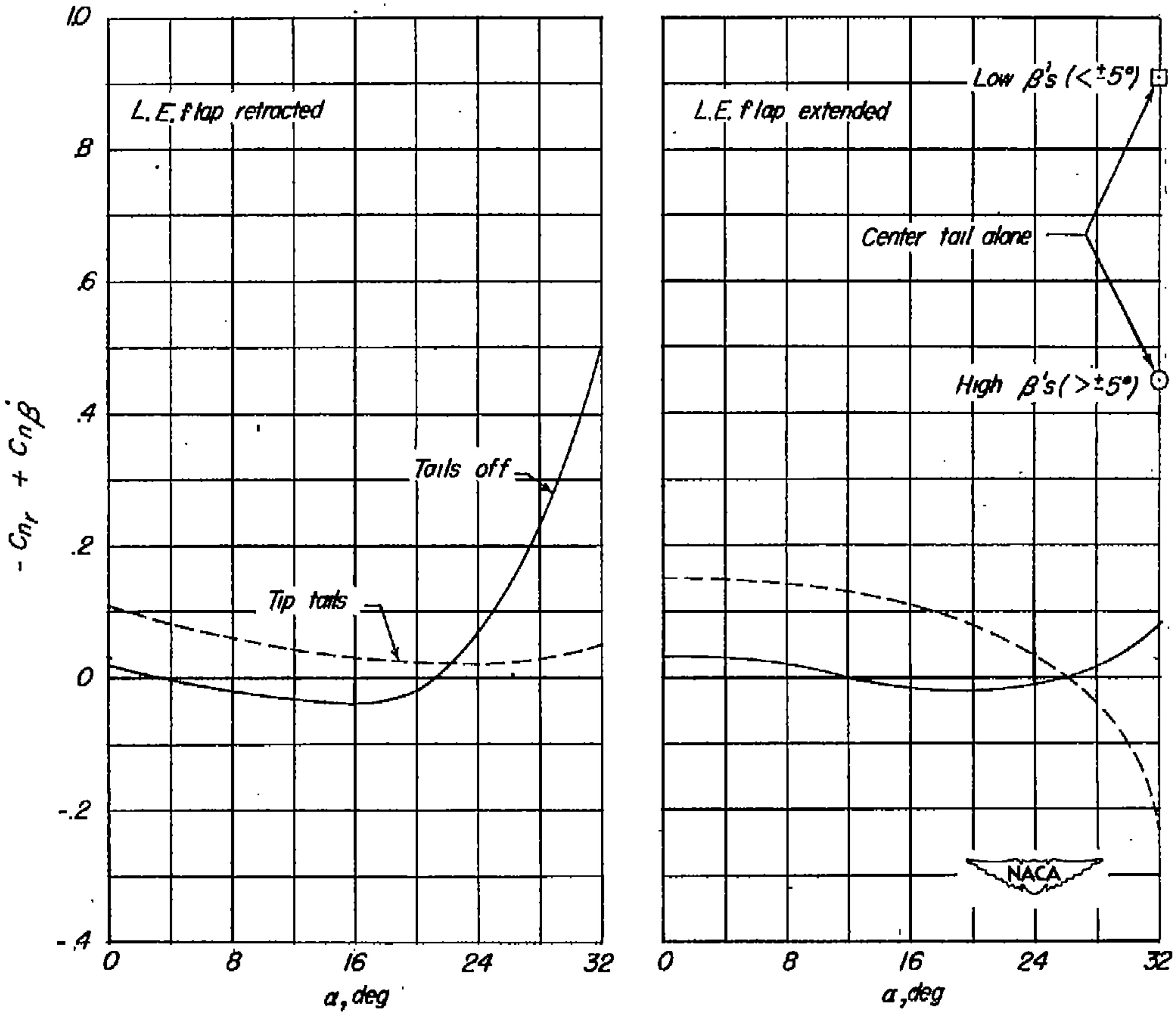

Figure 12.- Damping-in-yaw characteristics of model.

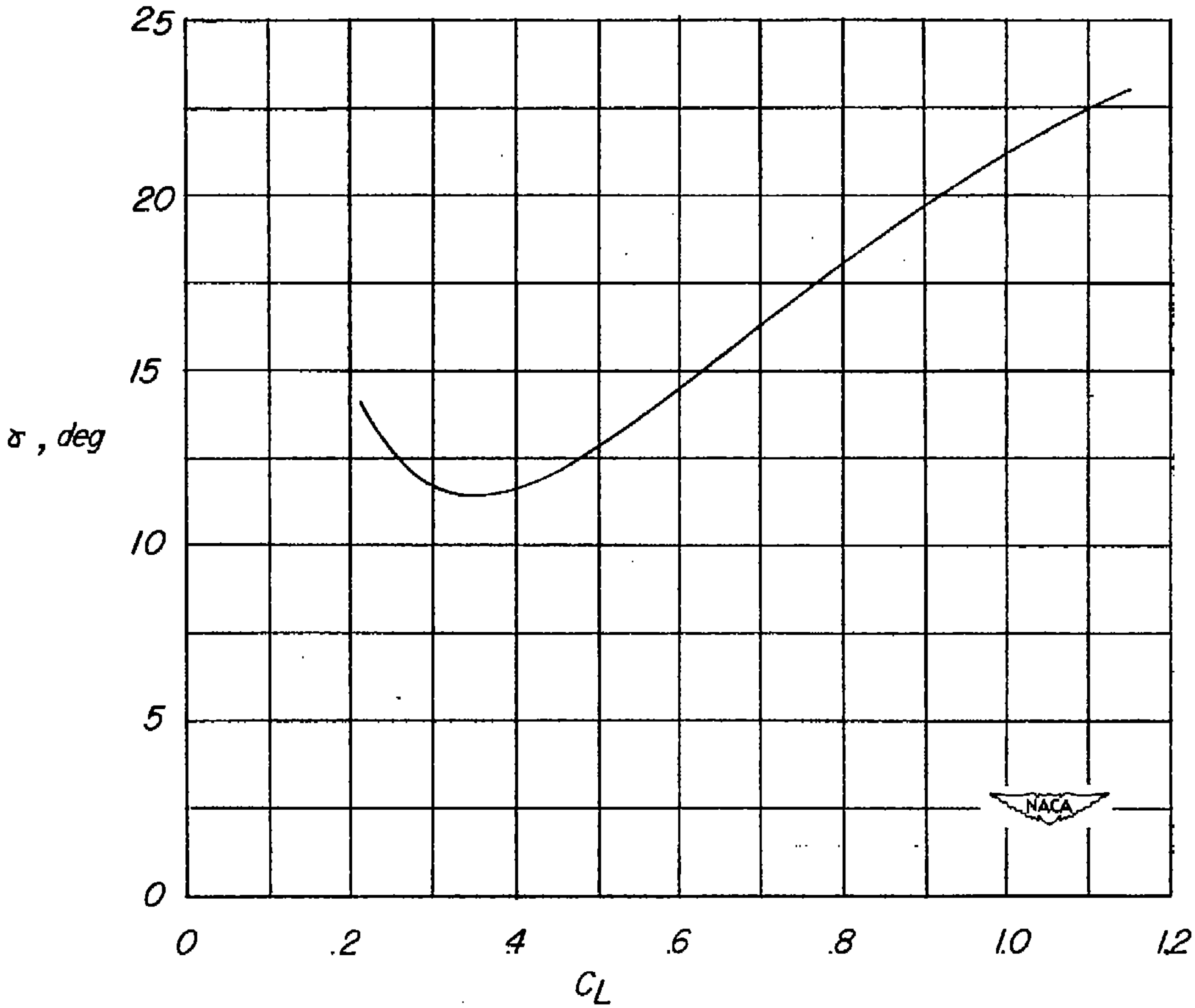

Figure 13.- Variation of glide-path angle with lift coefficient.